

MILIS: Multiple Instance Learning with Instance Selection

Zhouyu Fu, Antonio Robles-Kelly, *Senior Member, IEEE*, and Jun Zhou, *Member, IEEE*

Abstract—Multiple instance learning (MIL) is a paradigm in supervised learning that deals with the classification of collections of instances called bags. Each bag contains a number of instances from which features are extracted. The complexity of MIL is largely dependent on the number of instances in the training data set. Since we are usually confronted with a large instance space even for moderately sized real-world data sets applications, it is important to design efficient instance selection techniques to speed up the training process without compromising the performance. In this paper, we address the issue of instance selection in MIL. We propose MILIS, a novel MIL algorithm based on adaptive instance selection. We do this in an alternating optimization framework by intertwining the steps of instance selection and classifier learning in an iterative manner which is guaranteed to converge. Initial instance selection is achieved by a simple yet effective kernel density estimator on the negative instances. Experimental results demonstrate the utility and efficiency of the proposed approach as compared to the state of the art.

Index Terms—Multiple instance learning, support vector machine, feature selection, alternating optimization.

1 INTRODUCTION

MULTIPLE instance learning (MIL) is a paradigm in supervised learning proposed by Dietterich et al. [1]. It provides a framework for the classification of collections of instances called bags instead of individual instances. In a typical binary MIL problem, the training data are presented in the form of bags and their associated binary labels. The key assumption in MIL is that a negative bag only consists of negative instances, whereas a positive bag is comprised of both positive and negative instances, although the size of the bags can vary. Mathematically, this can be interpreted as taking the maximum over the labels of all instances in the bag given 1 as the label for the positive class and -1 as the label for the negative class. The hidden nature of the instance labels poses great challenges for MIL. In many cases, negative instances may even dominate in a positive bag. As a result, applying conventional supervised classification methods directly to MIL problems often leads to a downgraded performance [2]. Hence, special-purpose methods have to be designed to handle the MIL problems making use of the structure of MIL.

Many problems in computer vision and machine learning can be naturally cast in an MIL setting. For instance, in contents-based image retrieval (CBIR) [3], each image contains many regions, but only those that carry category-specific information are regions of interest (ROI) for

purposes of recognition. An ROI can either be a target object in the scene or a region describing the context of the object provided that it is relevant in the determination of the desired image class. Other regions may be shared across different categories and therefore possess no discriminative power. From this viewpoint, an image is a bag and the image regions are instances of the CBIR problem. MIL techniques can also be used for image-level image labeling, where a feature vector can be extracted at each pixel and a label is assigned to the whole image aggregating the information gathered from pixel level.

One potential problem that hinders the efficiency of MIL is the possible large number of instances encountered in real-world applications. For ROI-based image retrieval and object recognition, the training data set may consist of a large number of images, and each image may also contain many ROIs corresponding to the instances; thus, the total number of instances involved during the training stage could be prohibitively large. By the assumption of MIL, many instances in the positive class are background instances from the negative class and hence do not contribute much to discrimination. How to efficiently and effectively prune the large set of instances and keep the useful ones still remains a challenging problem for MIL.

In this paper, we propose an MIL method with instance selection (MILIS). The proposed algorithm is efficient in training and well suited for large-scale MIL problems. The method presented here has three major advantages. First, it employs an efficient and robust method for instance selection based on the distribution of negative instances. Second, it uses a single instance representation for each bag, similarly to MILES [4], albeit with much reduced dimensionality. This is mainly due to the use of a chosen subset of instances for bag-level feature computation in contrast to the use of all training instances, as in MILES [4]. The classifier is then optimized by intertwining instance selection with classifier learning in an alternating optimization framework, which is guaranteed to converge. Third,

- Z. Fu is with the Gippsland School of IT, Faculty of Information Technology, Monash University, Building 4N, Northways Road, Churchill, Victoria 3842, Australia. E-mail: zhouyu.fu@monash.edu.
- A. Robles-Kelly and J. Zhou are with the National ICT Australia, Canberra Research Laboratory, PO Box 8001, Canberra ACT 2601, Australia, and the College of Engineering and Computer Science, Australian National University. E-mail: {antonio.robles-kelly, jun.zhou}@nicta.com.au.

Manuscript received 21 Apr. 2009; revised 16 Nov. 2009; accepted 26 June 2010; published online 17 Aug. 2010.

Recommended for acceptance by J. Winn.

For information on obtaining reprints of this article, please send e-mail to: tpami@computer.org, and reference IEEECS Log Number TPAMI-2009-04-0251.

Digital Object Identifier no. 10.1109/TPAMI.2010.155.

due to the reduced complexity of the algorithm, for the data sets under study, the resulting classifier achieves comparable classification accuracies while being more efficient than alternative SVM-based classifiers for MIL.

The rest of the paper is organized as follows: In Section 2, we review the relevant MIL literature. We outline the important issues related to the topic and examine the limitations of the existing approaches. In Section 3, we formally define the notation for the proposed MILIS algorithm. The details of the algorithm are then elaborated upon in Section 4 by introducing the key components of MILIS and showing their integration into an iterative framework. Extension of the algorithm to multiclass settings and a computational complexity analysis are described in Section 5. To illustrate the efficiency and effectiveness of the proposed approach, in Section 6 we report the experimental results on four synthetic and real-world data sets. Finally, we draw conclusions in the last section of the paper and discuss future work on this topic.

2 RELATED WORK

Many methods have been proposed to solve MIL problems. These methods can be roughly divided into two main categories—generative and discriminative approaches. Generative approaches dominate in early attempts at tackling MIL problems, which aim at locating a region of interest in the instance feature space such that all positive instances lie in its vicinity and all negative instances are far removed from it. This can usually be cast in a maximum likelihood setting. Dietterich et al. [1] used axis parallel hyperrectangles to represent such regions with high positive probability. Maron and Lozano-Perez [5] proposed diverse density (DD), an elliptic target concept in feature space closely related to the peak density of positive instances. Zhang and Goldman [6] proposed EM-DD, an alternative to DD using the EM algorithm to locate the target concept in a more efficient manner. This was further generalized to GEM-DD by Rahmani et al. [7], which keeps multiple hypotheses of the target concepts, and hence can achieve improved robustness in locating them.

MIL problems can also be tackled in a discriminative manner aiming at adapting standard supervised learning approaches. For instance, citation K-nearest neighbor (KNN) [8] extends the standard KNN classifier to MIL by employing the K-neighbors at both the bag and instance levels. Other variants hinge in the use of support vector machine (SVM) classifiers [9], which result in a plethora of SVM-based methods for MIL, which include MI-kernel [10], MI-SVM [11], mi-SVM [11], DD-SVM [3], MILES [4], and other instance level SVM formulations [12], [13], [14]. Other classifiers that generalize the single instance counterparts above can also be adopted. These include MI-Boosting [15], MI-Winnow [16], and MI logistic regression [2], [17].

Alternatively, we can divide the existing approaches to MIL into top-down and bottom-up ones. Top-down approaches try to infer the bag label directly. During the inference process, additional cues can be gathered to infer the instance labels in a further inference step [4]. Bottom-up approaches work by first inferring the instance labels and then resolving those corresponding to the bags. Generative approaches to MIL are normally bottom-up in nature since

the inference process is often effected in the instance feature space. Discriminative approaches, on the other hand, are mostly top-down ones addressing bag-level predictions directly. An alternative to this approach is the mi-SVM [11] and akin methods [12], [13] that perform instance inference directly through a generalization of the maximum margin rationale used in SVMs.

The main argument leveled against the bottom-up generative approaches is the use of single or a limited number of prototypes to represent the target concepts for the positive class. Despite their empirical success, DD-based approaches rely on a strong assumption that all positive instances form a compact cluster in the feature space. This cluster is exclusive with respect to the collection of negative instances. This is, however, not necessarily the case in real applications as the distributions of positive instances can be arbitrary and, most likely, multimodal. Hence, a single target concept in the feature space may be insufficient for capturing the distribution of the positive class. Methods such as DD-SVM [3] and GEM-DD [7] remedy this problem by employing multiple prototypes obtained with different start values through iterative optimization approaches. This motivates our observation that multiple prototypes can be formed and updated iteratively. This delivers robustness to perturbations in the instance feature space due to the aggregation of instance-level reasoning.

3 PRELIMINARIES AND ALGORITHM OVERVIEW

To describe MILIS, we need to introduce some notation. Denote $\mathcal{X}^{\text{tr}} = \{X_1, \dots, X_n\}$ as the set of bags and $Y^{\text{tr}} = \{y_1, \dots, y_n\}$ as the labels associated with each bag. A bag X_i contains m_i instances denoted by $\mathbf{x}_{i,j}$ for $j = 1, \dots, m_i$. Without ambiguity, $\mathbf{x}_{i,j}$ also denotes the feature vector for the instance depending on the context. Different bags can have different numbers of instances; hence, m_i may vary for different bags. Each instance $\mathbf{x}_{i,j}$ is also associated with a label $y_{i,j}$, which is not directly observable. The assumption is that all instances in negative bags are negative and at least one instance is positive in each positive bag. The purpose is therefore to predict the label value for the novel test bag $X = \{\mathbf{x}_1, \dots, \mathbf{x}_n\}$.

With the above ingredients, we can now describe the MILIS framework for MIL. We first focus on the binary classification case, where the label value $y_i \in \{-1, 1\}$ for each bag i , where $y_i = 1$ if the bag indexed i corresponds to the positive class and $y_i = -1$ otherwise. By just a few minor modifications, we will later generalize the framework to handle multiclass MIL problems. The basic steps of the MILIS algorithm are illustrated in Fig. 1, where each block represents an object to operate on. Each arrow indicates an operation defined on the objects. In the training phase, we first perform instance selection on the training instances. This is achieved by modeling the distributions of negative instances and picking the least negative one from each positive bag. After doing this, we obtain a set of instance prototypes (IPs), which we denote by $x_i^{*(t)}$. Each of these is chosen from the corresponding positive bag. We then convert the MIL problem into a single instance problem via a similarity-based feature mapping using the selected IPs. A single feature vector is formed per bag. In the figure, z_i

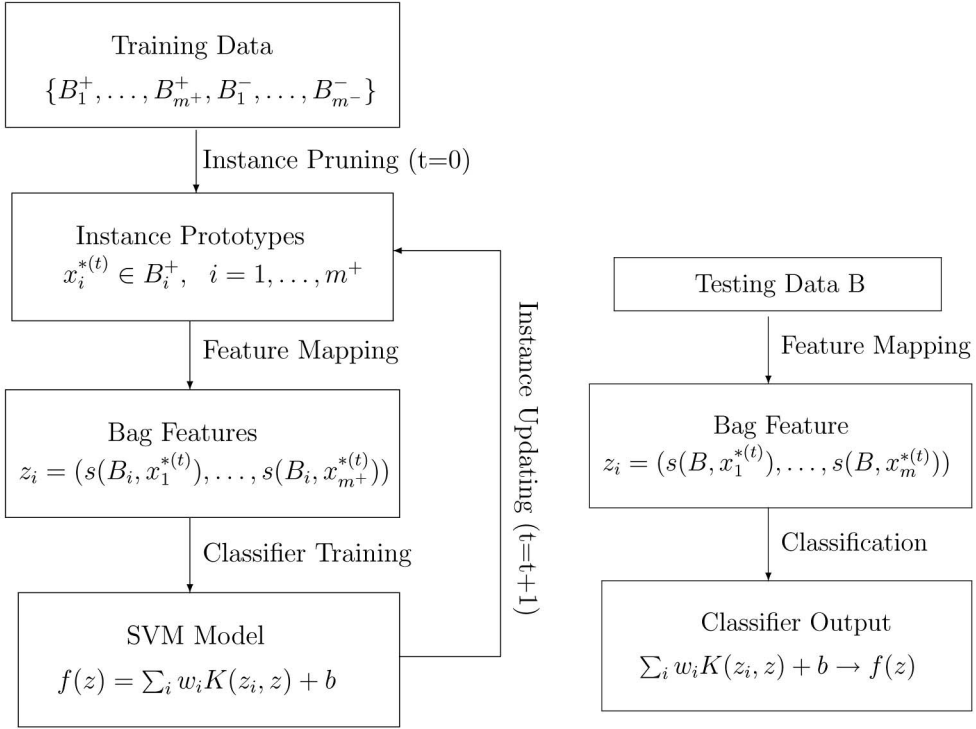


Fig. 1. Block diagram for the proposed algorithm. Left-hand column: training phase; right-hand column: testing phase.

denotes the computed feature vector for the i th bag and $s(B_i, x_j^{*(t)})$ denotes the j th feature element which captures the similarity between bag B_i and instance $x_j^{*(t)}$. The explicit form of $s(B_i, x_j^{*(t)})$ will be given in the context that follows. This feature map is in accordance with the single instance feature representation proposed by MILES [4]. Given the bag-level feature vectors, a standard linear SVM classifier is trained on the bag features. Based on the classification results on the training data, we update and reselect the IPs. This step sequence is interleaved until convergence.

In the testing phase, we commence by extracting the feature vector for the test bag using the feature mapping defined over the IPs obtained in the training phase. The trained SVM classifier is then applied so as to obtain the classification result.

It is worth noting that instance selection has been addressed previously in a different context. SVM-based approaches to MIL such as MI-SVM and mi-SVM [11] perform instance selection to train an SVM classifier in the instance feature space. In contrast, the proposed MILIS algorithm employs instance selection to form the single instance feature representation at the bag level. In this way, the original MIL problem is converted into a prototype selection one. Thus, the purpose of instance selection in MILIS is to construct a more discriminative feature map for learning bag-level classifiers, whereas MI-SVM and mi-SVM aim at selecting the true positive instances for learning instance-level classifiers.

4 INSTANCE SELECTION AND CLASSIFIER LEARNING

In this section, we present the foundations of MILIS. Like MILES [4], our method aims at solving bag labels directly

without resorting to instance-level learning in the training process. Note that MILES [4] directly constructs bag-level features based on bag-to-instance distances. Each instance is used to form the bag-level feature mapping and treated as a potential target concept carrying category information, which we term IP in the context that follows. This gives rise to a very high-dimensional feature vector whose dimensionality is given by the total number of instances. Feature selection on these vectors is done implicitly via a one-norm linear SVM, which is known to produce sparse solutions for feature weights [18]. Although effective, MILES has difficulty scaling up to large data sets due to the fact that the dimensionality of the instance feature space is given by the sum of all instances across all bags, and hence grows linearly with respect to the number of training instances. This leads to high complexity for both feature computation and one-norm SVM optimization.

To achieve comparable performance to MILES with much less computational complexity, explicit instance pruning and selection is necessary. Hence, a principled way is required to reduce complexity devoid of clustering or quantization procedures. This is an important observation since clustering and quantization do not consider bag-level structure or discriminative information, and may discard small clusters in the feature space where informative features may be located. Hence, we adopt a similar feature representation as MILES, which will be described below, and, at the same time, the importance of instance pruning for efficient MIL is highlighted. We then propose a novel discriminant pruning scheme based on density estimation. Next, the problems of feature learning and instance updating are addressed. Finally, we summarize the

algorithm and provide some theoretical study on its property and computational complexity.

4.1 Bag-Level Feature Representation

To effectively employ the similarity-based feature mapping in Fig. 1, a distance metric needs to be defined first between bags and instances. The Hausdorff distance is a natural distance metric for this purpose. Specifically, the distance between bag B_i and instance \mathbf{x} is given by

$$d(B_i, \mathbf{x}) = \min_{\mathbf{x}_{i,j} \in B_i} \|\mathbf{x}_{i,j} - \mathbf{x}\|^2, \quad (1)$$

which is the distance between x and its nearest neighbor in B_i .

Given the distance metric above, we can then derive the following similarity measure using an exponential function:

$$s(B_i, \mathbf{x}) = \exp(-\lambda d(B_i, \mathbf{x})) = \max_{\mathbf{x}_{i,j} \in B_i} \exp(-\gamma \|\mathbf{x}_{i,j} - \mathbf{x}\|^2). \quad (2)$$

If instance x is a true positive instance, then a positive bag should have high similarity to instance x . A negative bag, on the other hand, has a low similarity since all instances in the negative bag are far apart from x .

Recall that MILES uses all instances in the training set directly to construct the bag-level feature vector. The resulting feature vector for bag i is an m -dimensional vector comprised by the concatenated bag-to-instance similarities:

$$\mathbf{z}_i^{\text{MILES}} = [s(B_i, x_{1,1}), \dots, s(B_i, x_{1,m_1}), \dots, s(B_i, x_{n,1}), \dots, s(B_i, x_{n,m_n})], \quad (3)$$

where $m = \sum_{i=1}^n m_i$ is the total number of instances in the training data set. The subset of input instances is then selected indirectly by solving a one-norm sparse linear SVM and eliminating the feature dimensions corresponding to zero classifier weights.

Despite its flexibility and robustness, the above feature mapping scheme often leads to a computationally expensive training process. The reasons are twofold. First, the feature mapping results in full-length features, whose dimensionality is given by the total number of instances in the training set. Even for moderately large data sets, this could still be a large number. Furthermore, the feature matrix is not sparse. In order to calculate a single entry of the feature matrix, a nearest neighbor search between features of the prototype instance and those in the bag under study is required. This consumes not only many computational resources but also a lot of storage. Second, there is no efficient method to solve the one-norm SVM except from solving its linear programming (LP) formulation. This becomes the bottleneck in the efficiency of the MILES. For some large-scale MIL data sets, even commercial LP solvers can be very slow or even inapplicable. Thus, it would be desirable to design an alternative approach that can reduce the computations in both feature mapping and classifier learning, while at the same time, exploiting the single instance feature representation of MILES.

4.2 Initial Instance Selection

As discussed before, DD-based instance selection is computationally expensive as it involves solving an unconstrained optimization problem for every instance in the training set in order to recover all the prototypes

corresponding to the DD extrema. Instead of using all training instances to form the bag-level feature vector in (3), DD-SVM chooses a set of prototypes to construct the feature map. The prototypes are obtained by running EM-DD [6] from different initial points.

In this section, we propose an efficient approach to instance selection for the construction of bag-level feature map. We select existing instances in the training set to construct the similarity-based feature. This is equivalent to taking columns of the MILES feature representation in (3). To construct bag-level feature vectors, a single instance is selected from each training bag to form the subset of IPs for feature mapping. Intuitively, we want to include true positive and negative instances in the subset to compute a discriminative feature map. Note that following the MIL assumption, everything in the negative bag is negative. Hence, the key problem here is to locate the true positive instances. While DD-based selection approaches try to consider true positive instances directly and attempt to locate regions in the feature space with high positive density, it is much more effective to model the distribution of the negative population. Since negative instances can have very general distributions, to model all instances contained in the negative bags we use the following Gaussian-kernel-based kernel density estimator (KDE) [19]:

$$f(x) = \frac{1}{Z \sum_i m_i} \sum_{y_i=-1} \sum_{j=1}^{m_i} \exp(-\beta \|x - x_{i,j}^-\|), \quad (4)$$

where $x_{i,j}^-$ denotes the j th instance from the i th negative bag, Z is a normalization factor making $f(x)$ a proper density. It is constant over the instance space, and thus is ignored in our calculation. We have employed an isotropic Gaussian kernel with the scale parameter β controlling the range of influence for training instances. Note that the above equation defines a normalized probability density function (PDF) for the negative population.

The major advantage in modeling the negative population in this manner resides in the fact that, due to their large quantities, negative instances usually dominate the joint PDF in MIL settings. Their distributions can then be modeled more accurately than true positives making use of KDE. To achieve an efficient density estimation for each positive instance, we pick its K-nearest negative instances and evaluate the probability of the positive instance being generated from the negative population via (4). The search process can be accelerated by using the approximate KNN search method in [20]. We then pick the single instance with the lowest likelihood value, i.e., the least negative instance, from each positive bag as the IP. For each negative bag, on the other hand, we pick the single instance with the highest likelihood value, i.e., the most negative instance, as the IP used in the feature mapping. The total number of IPs obtained is equal to the number of bags. This compares quite favorably with the number of prototypes used in MILES, which is equivalent to the set of all training instances. This results in a much lower dimensional feature space without much loss of discriminatory power, as each bag is represented by a corresponding instance selected from the bag. Compared to DD-based selection, we also obtain improved IPs in a more computationally efficient

manner. Furthermore, since our instance selection method is governed by PDFs, it is more robust to noise corruption and outliers in the data set. Finally, as we will see later, the above instance selection procedure can be generalized to the multiclass MIL case. The complexity is solely determined by the number of instances and is independent of the number of classes.

4.3 Classification

After initial instance selection, we have obtained a subset of instance prototypes $\{x_1, \dots, x_n\}$, where x_i is the prototype selected from the i th bag in the training set. The bag-level feature is then given by

$$\mathbf{z}_i = [s(B_i, x_1), \dots, s(B_i, x_2), \dots, s(B_i, x_n)], \quad (5)$$

where $s(B_i, x_j)$ is computed via (2). We then train a classifier that can be applied to the bag features. To this end, we use linear SVM, which employs the L_2 norm for both the regularization term on feature weights \mathbf{w} and the data term as follows:

$$\begin{aligned} f(\mathbf{w}) &= \frac{1}{2} \|\mathbf{w}\|^2 + C \sum_i \ell(y_i, \mathbf{w}^T \mathbf{z}_i), \\ \ell(y_i, \mathbf{w}^T \mathbf{z}_i) &= (1 - y_i \mathbf{w}^T \mathbf{z}_i)_+, \end{aligned} \quad (6)$$

where $y_i \in \{-1, 1\}$ is the label value for bag i , C is the regularization parameter that controls the influence of the second term on the right-hand side of the above equation. The resulting classifier is given by $\mathbf{w}^T \mathbf{z}$, where \mathbf{w} are the linear weights for the features. Here, we have also absorbed the bias term into the weight vector \mathbf{w} for the sake of simplicity. $\ell(y_i, \mathbf{w}^T \mathbf{z}_i)$ specifies the loss function for classification, where $(v)_+ = \max(0, v)$ is the Hinge loss normally adopted for SVM classifiers.

The reason for the use of L_2 linear SVM here corresponds to computational efficiency. Unlike one-norm SVMs, which are solved by standard linear programming optimization routines and do not scale up with training sample sizes, two-norm SVMs have been well studied in the literature. There are fast routines to solve the underlying quadratic program for two-norm SVMs [21], [22] using linear and nonlinear kernels. Linear SVMs can be trained in an efficient manner using various methods proposed in the literature [23], [24]. Note that we can also use a nonlinear SVM classifier here. Nonetheless, there are several advantages to using linear SVMs aside from efficiency alone. First, linear SVMs can be used for implicit feature selection. We can discard feature dimensions with small coefficients in the classifier weight \mathbf{w} , thus effectively further reducing the number of instances used in constructing the feature mapping. SVMs with nonlinear kernels such as the RBF one do not have this property for feature selection. All feature dimensions are treated equally in the computation of nonlinear kernels. Second, the feature mapping defined in (5) is itself nonlinear in nature due to the use of an exponential operator that maps distances to similarities. It defines a higher dimensional embedding in the original feature space via this nonlinear mapping. Consequently, a linear classifier suffices to separate features which are not linearly separable in the original feature space.

4.4 Instance Update

After obtaining the SVM classifier for bag-level features, we can validate the selected IPs and update them accordingly. This can be cast as an optimization problem over discrete variables that can be efficiently solved using an approach akin to coordinate descent. To introduce the optimization problem, we define a set of auxiliary variables ϕ_i , where $i = 1, \dots, n$, for each bag in the training set. Each ϕ_i can take values in $\{1, \dots, m_i\}$ and $\phi_i = j$ implies that the j th instance in the i th positive bag is selected as the IP for the feature mapping. With these ingredients, we now define the optimization problem underlying the iterative framework in terms of the variables ϕ_i and the classifier weights \mathbf{w} as follows:

$$\begin{aligned} \min_{\mathbf{w}, \phi} Q(\mathbf{w}, \phi) &= \frac{1}{2} \|\mathbf{w}\|^2 + C \sum_i \ell(y_i, \mathbf{w}^T g(B_i, \phi)), \\ g(B_i, \phi) &= [s(B_i, \mathbf{x}_{1,\phi_1}), \dots, s(B_i, \mathbf{x}_{n,\phi_n})], \end{aligned} \quad (7)$$

where $\ell(y_i, f_i)$ is the same loss function as defined in (6) and $g(B_i, \phi)$ specifies the bag-level feature mapping for the i th bag B_i given the indices of the prototypes $\phi = \{\phi_1, \dots, \phi_n\}$. Given the trained SVM classifier with weights \mathbf{w} , we can further update the IP for each bag. This is equivalent to minimizing $Q(\mathbf{w}, \phi)$ in (7) with respect to ϕ . We adopt a reminiscent procedure of coordinate descent so as to update ϕ_i for each bag as follows:

$$\begin{aligned} \phi_1^{(t+1)} &= \arg \min_{j=1}^{m_1} \sum_i \ell(\mathbf{w}^T g(B_i, \{j, \dots, \phi_n^{(t)}\}), y_1), \\ &\dots \\ \phi_i^{(t+1)} &= \arg \min_{j=1}^{m_i} \sum_i \ell(\mathbf{w}^T g(B_i, \{\dots, \phi_{i-1}^{(t)}, j, \phi_{i+1}^{(t)}, \dots\}), y_i), \\ &\dots \\ \phi_n^{(t+1)} &= \arg \min_{j=1}^{m_n} \sum_i \ell(\mathbf{w}^T g(B_i, \{\phi_1^{(t)}, \dots, j\}), y_n), \end{aligned} \quad (8)$$

where $\phi_i^{(t)}$ and $\phi_i^{(t+1)}$ correspond to the old and updated index values for the i th bag, respectively, \mathbf{w} is fixed to $\mathbf{w}^{(t)}$ for the t th iteration. Since \mathbf{w} is unchanged during the update of ϕ , only the second term on the right-hand side of (7), i.e., the data term of the SVM objective function, is considered here. Each ϕ_i is updated while fixing all other ϕ 's. We can see that each update of the IPs leads to a lower cost for the SVM data term, and hence, decreased upper bound on the classification error. The order in which the IPs are updated is not fixed and can be shuffled randomly. Here, we choose an ordering scheme such that IPs for misclassified bags are updated first. In our experiments, this scheme has delivered good performance.

Despite the simple procedure of the instance update algorithm, a naive implementation may lead to a very time-consuming computational process. This involves calculating the bag-to-instance affinity between each bag in the training set and every training instance except those currently chosen as the IPs. This has the same time complexity as computing the full MILES feature embedding. Thus, following each such update, the bag-level

$$(Z^{(t+1)}, \phi^{(t+1)}) = \text{instupdate}(B, Y, Z^{(t)}, \phi^{(t)}, \mathbf{w})$$

$$(Z^{(t+1)}, \phi^{(t+1)}, v) \leftarrow (Z^{(t)}, \phi^{(t)}, 0)$$

foreach Bag $i = 1, \dots, n$ **do**

$$f_i = \mathbf{w}^T Z_i^{(t)}$$

$$v = v + \ell(y_i, f_i)$$

end

foreach Bag i with $\ell(y_i, f_i) > 0$ **do**

foreach Instance j in bag i and $j \neq \phi_i$ **do**

$$(v', p', f') = \text{feature_update}(x_{i,j}, Z_{:,i}^{(t)}, \mathbf{w}, f, v)$$

if $v' < v$ **then**

$$(Z_{:,i}^{(t+1)}, \phi_i^{(t+1)}, v, f) \leftarrow (p', j, v', f')$$

end

end

end

$$(v', p', f') = \text{feature_update}(x, Z_{:,j}, \mathbf{w}, f, v)$$

$$v' = 0$$

foreach Bag i **do**

$$p'_i = S(B_i, x) \text{ via Equation 2 } f'_i = f_i + w_j(z'_{i,j} - z_{i,j}) \quad v' = v' + \ell(y_i, f_i)$$

if $v' \geq v$ **then**

quit with $v' = \inf$

end

end

Fig. 2. Pseudocode for instance update.

feature values are changed. This implies that the decision values need to be reevaluated for each training example.

Fortunately, we can avoid the above computationally expensive steps by taking advantage of the incremental nature of the instance update process. We make use of two important observations here. First, the update of each ϕ_i would result in the change of the i th feature element for the bag-level feature mapping, while all other feature dimensions are unaffected. Hence, instead of recalculating the classifier output for the new feature vector, we can update the classifier output incrementally based on the change in the i th feature alone. Second, empirical observations show

that only a few training instances are discriminant for the MIL problems we are studying. This is especially true for the case of positive bags with many instances in which the majority of the instances are false positives bearing little discriminant information. Hence, many training instances, if chosen as prototypes, will contribute to a higher cost function value. Therefore, we can update the feature map and the classifier output simultaneously and stop the update process early on if the new feature map yields solutions that depart from the current optimum.

The pseudocode of the instance update algorithm can be found in Fig. 2, where $B, Y, Z^{(t)}, \phi^{(t)}$, and \mathbf{w} are the training

Input: the set of training bags $(B_1^+, \dots, B_{m^+}^+, B_1^-, \dots, B_{m^-}^-)$

- Initial instance selection by applying KDE in Equation 4 to instances in positive bags and extracting IPs
- Train an SVM classifier (Equation 6) on bag-level features obtained from the mapping in Equation 5 using the previously extracted prototypes
- Update IPs based on the learned SVM classifier via Equation 8
- Repeat the above two steps until convergence
- Remove instances with small feature weights and update the classifier.

Output: the set of chosen IPs indexed by ϕ_i 's and the SVM classifier $f(\mathbf{z}) = \mathbf{w}^T \mathbf{z}$ with weight \mathbf{w} .

Fig. 3. Summary of the proposed iterative framework for instance selection and classifier learning.

data, training labels, current feature map, indices of prototypes currently selected, and the classifier weights, respectively. The algorithm outputs the updated feature map $Z^{(t+1)}$ and the new indices of prototypes $\phi^{(t+1)}$. The basic flow of the algorithm should be self-explanatory from the pseudocode. The “feature_update” subroutine adopts the above-mentioned strategies within the for loop, where new classifier output ℓ'_i is updated from the current output ℓ_i and each iteration is stopped early if the cost function value v' for the new feature map (evaluated up to the current bag) is suboptimal with respect to the current value of v .

4.5 Iterative Learning Framework

The two steps of classifier training and instance selection can be interleaved in a two-step optimization fashion. Once a classifier is trained, we can update the IPs. Then, a new classifier can be learned from the updated feature mapping. This can be viewed as minimizing the optimization problem defined in (7) over continuous and discrete variables. The initial instance selection process discussed in Section 4.2 corresponds to the initialization of ϕ . While SVM training corresponds to optimization with respect to \mathbf{w} while fixing ϕ , the instance update process discussed in the previous section is equivalent to minimizing ϕ while fixing \mathbf{w} .

It is straightforward to see that each iteration decreases the value of the cost function in (7) according to the following relation:

$$f(\mathbf{w}^{(t)}, \phi^{(t)}) \leq f(\mathbf{w}^{(t+1)}, \phi^{(t)}) \leq f(\mathbf{w}^{(t+1)}, \phi^{(t+1)}), \quad (9)$$

where $\mathbf{w}^{(t)}$ and $\phi^{(t)}$ refer to the old classifier weights and the indices of prototypes in each bag, while $\mathbf{w}^{(t+1)}$ and $\phi^{(t+1)}$ correspond to new classifier weights and indices of IPs. The first inequality holds due to the classifier updating step and the second inequality arises from instance updating. Because of the monotonic decrease in energy, the iterative learning framework is guaranteed to converge in a finite number of steps. Moreover, since ϕ can only take a finite set of values

due to the discrete nature of the ϕ_i variables, this updating process is guaranteed to converge toward $\phi_i^{(t+1)} = \phi_i^{(t)}$ for every i . That is, at convergence, the IPs selected from two adjacent iterations do not change.

The above procedure is reminiscent of the EM algorithm [25], which aims at recovering maximum likelihood solutions to problems involving missing or hidden data by iterating between two computational steps. In the expectation (E) step, we estimate the a posteriori probabilities of the hidden data using maximum likelihood parameters recovered in the preceding maximization (M) step. The M-step in turn aims at recovering the parameters which maximize the expected value of the log-likelihood function. Despite their similarity, the underlying nature of the method proposed here and the EM algorithm are quite different. First, from the statistical point of view, the EM algorithm provides a means for maximum likelihood parameter estimation in the presence of hidden variables. In contrast, the target function in (7) for our method is tailored to the setting of the MIL problem being considered and is not related to the likelihood function or a particular expression of the a posteriori probabilities. Second, from the optimization point of view, the EM algorithm is well known as a bound optimization technique that maximizes a concave lower bound on the likelihood function at each iteration [26]. Our method, on the contrary, is a minimizer of the target function without resorting to a lower bound.

The step sequence of the iterative framework for instance selection and classifier learning is outlined in Fig. 3. In the algorithm above, after the SVM classifier is trained in the last iteration, we adopt a final feature pruning step by removing all features with small feature weights. Since these features have a small contribution to the final output of the linear classifier, the classification performance does not suffer from removing these redundant instance features. Specifically, the j th feature is removed if the magnitude of its corresponding feature weight is small, that is, $|w_j| < r$ for some small $r > 0$. The threshold r can best be determined relative to the scale of

the feature weights by some simple statistics, such as the mean and the median of the feature weights.

As we will see in Section 6, the performance of the proposed method is not sensitive to the choice of the value of r . Note that the strategy used here is similar to the recursive feature selection technique for SVM [27], which also uses feature weights obtained from the SVM classifier as indicators for their discriminabilities. Instead of removing a single instance feature and retraining the SVM at each iteration, we make use of the threshold r and prune multiple features in the space at every step of the algorithm. This final step results in further instance pruning by removing the indiscriminate instance prototypes as indicated by the classifier weights. Since each feature in the feature map corresponds to one selected prototype, after removing those redundant prototypes, the feature map can be updated and the SVM classifier retrained based on the updated instance feature matrix. In this way, we can improve on the efficiency of testing without influencing the performance, since prediction time is monotonic to the number of instances used to form the feature mapping.

The algorithm in Fig. 3 can also be formulated in a one-norm SVM framework simply by replacing the standard SVM classifier with the one-norm SVM classifier [18] in a similar fashion as MILES [4] and the one-norm extension of MI-SVM [14]. The training of the SVM classifier becomes a standard linear program and the instance update procedures can also be modified accordingly. With the one-norm formulation, feature selection can be achieved in an implicit manner since the L_1 norm imposes sparsity on the learned feature weights. However, two major disadvantages hinder our further consideration of this alternative. First, it may still be computationally expensive to solve the linear program arising from the one-norm formulation, whose complexity scales with the number of bags in the training set. It may be costly to solve the new one-norm SVM formulation if the MIL problem contains a large number of bags. However, this is not a problem for SVMs with squared norms, where there exist efficient methods for training on large data sets [21], [22]. Second and more important, one-norm SVM, despite its ability for implicit variable selection, does not have any advantage in performance over the standard SVM when incorporated into our MILIS framework. It is worth noting that in our empirical evaluation of MILIS using both standard and one-norm SVMs on the benchmark MUSK and COREL data sets, as mentioned in Section 6, one-norm SVM delivers inferior classification performances as compared to those produced by squared-norm SVMs. Hence, we still focus on the standard SVM formulation and resort to an additional step of final feature pruning to maintain the sparsity of the obtained IPs as discussed above.

In the testing stage, given a test bag B , we first form its bag-level feature vector \mathbf{z} via (5) using the learned IPs. Prediction is made by taking the sign of the decision value output the linear SVM:

$$\begin{aligned} \mathbf{z} &= [s(B, x_1), \dots, s(B, x_2), \dots, s(B, x_n)], \\ f(B) &= \text{sgn}(\mathbf{w}^T \mathbf{z}). \end{aligned} \quad (10)$$

5 EXTENSION TO THE MULTICLASS SETTING

In this section, we show how the algorithm proposed in the previous sections for binary MIL can be generalized to handle multiclass MIL tasks. Unlike traditional approaches that make use of various classifier fusion frameworks to decompose the multiclass problem into several binary ones and combine the results from the binary classifiers for multiclass classification [28], [29], we propose solving the multiclass MIL problem using a direct formulation of the SVM for multiclass classification problems [30]. For the binary MIL algorithm based on instance selection discussed above, this can be effectively achieved by making some minor modifications as described below.

5.1 Instance Selection

For multiclass MIL problems, each class is a positive one against the remaining classes. Hence, for each bag in any class, there exists at least one true positive instance carrying the discriminant information for the class under consideration where the remaining instances may be viewed as “background” ones. For some applications, there might be a number of bags that contain background instances alone, akin to the negative class in the binary case. Note that this change in the problem formulation does not influence our instance selection framework. The reason for this will soon be apparent.

We still use density estimation to evaluate the conditional probability for the distributions of instances for each class. Yet, instead of treating them as the true positive distributions for themselves, we use the class conditional distribution of each class to model the negative distributions for other classes. Denote by $P(x|\Omega_k)$ the class conditional distribution of training instances from the k th class. An estimate of $P(x|\Omega_k)$ can be obtained from kernel density estimation via (4) over all instances extracted from the k th class. Again, in estimating the conditional probabilities of novel instances for the j th class, we first perform a K-NN search to find an appropriate neighborhood in the j th class before applying (4) for density evaluation. With the class conditional probability values at hand, we then use the following likelihood ratio value defined for the j th instance in the i th bag, $x_{i,j}$, as an indicator for its discriminability:

$$r(x_{i,j}) = \frac{P(x_{i,j}|\Omega_{y_i})}{\max_{k \neq y_i} P(x_{i,j}|\Omega_k)}, \quad (11)$$

where $y_i \in \{1, \dots, c\}$ is the label for bag i .

The instance with the largest likelihood ratio value in the above equation is selected as the initial prototype for bag i . That is, $\phi_i^{(0)} = \arg \max_j r(x_{i,j})$. This is similar to the binary case. The main difference is in the modeling of the negative distribution for each class. We take the maximum over all other classes for two reasons. First, this is more efficient than running the density estimator over all instances from all other classes. As a result, we end up running KDE for each class only once. Second, the maximum of the class conditional probability is a robust indicator for the discriminability. If and only if all other classes have a low density and the current class has a high density over the support region of the instance can the instance become a prototype that carries

the discriminative information for the class it represents. Thus, our multiclass selection strategy provides a seamless way to handle different classes. More importantly, the feature map inferred from the selected IPs is common for all different classes, which makes the following classifier learning and optimization process more convenient.

5.2 Classification

Crammer and Singer [30] have proposed a multiclass SVM by solving the following single optimization problem:

$$\begin{aligned} \min f(\mathbf{w}_1, \dots, \mathbf{w}_c) &= \sum_{j=1}^c \frac{1}{2} \|\mathbf{w}_j\|^2 + C \sum_i \ell(y_i, f_i) \\ \ell(y_i, f_i) &= (1 - (f_{i,y_i} - \max_{j \neq y_i} f_{i,j}))_+^2. \end{aligned} \quad (12)$$

Here, c linear classifiers are learned in parallel and $f_i = [f_{i,1}, \dots, f_{i,c}]$ are the decision values returned by the c linear classifiers. The weight for the k th linear classifier is given by \mathbf{w}_k and $f_{i,k} = \mathbf{w}_k^T \mathbf{x}_i$ is the decision value returned by the k th classifier. A testing example is assigned label k if the decision value returned by the k th classifier is larger than those returned by other classifiers.

In the above equation, $\ell(y_i, f_i)$ represents the generalized squared Hinge loss for multiclass output, which vanishes if and only if $f_{i,y_i} - \max_{j \neq y_i} f_{i,j} \geq 1$. The use of $L_+(\cdot)$ encourages large margins over wrong decisions for the training data. The second term on the right-hand side specifies an upper bound on the classification error, whereas the first term is the regularization term that penalizes complicated decision boundaries.

5.3 Instance Update

The step sequence of the instance update algorithm remains the same as that presented in Fig. 2 except for two minor changes. First, the binary hinge loss term $L(f_i, y_i)$ is represented by its multiclass counterpart $L(f_{i,1}, \dots, f_{i,c}, y_i)$, as defined in (12). Second, the two equations for evaluating and updating classifier output values f_i in the “feature_update” routine are replaced by the following two equations:

$$\begin{aligned} f_{i,k} &= \mathbf{w}_k^T Z_i^{(t)}, \\ f'_{i,k} &= F_{i,k} + w_{j,k}(z'_{i,j} - z_{i,j}), \end{aligned}$$

and an additional loop is added to evaluate $f_{i,k}$ and update $f'_{i,k}$ for all $k = 1, \dots, c$.

For the final instance pruning after the iterative update of instance prototypes and classifiers, pruning is effected if and only if the corresponding instance feature weights for all c classifiers are small. Note that the testing stage shares the same first step as in the binary case. The bag-level feature vector \mathbf{z} is formed via (5) using the learned IPs. The bag is then assigned the label corresponding to the largest decision value output by the linear SVM

$$f(B) = \arg \max_{j=1}^c \mathbf{w}_j^T \mathbf{z}, \quad (13)$$

where $\mathbf{z} = [s(B, x_1), \dots, s(B, x_2), \dots, s(B, x_n)]$.

6 EXPERIMENTAL RESULTS

We performed experiments on both synthetic data and real-world data sets to demonstrate the utility of the proposed

algorithm. We use synthetic data to show the effectiveness of the MILIS algorithm in instance selection and compare it against EM-DD-based selection criteria [6], [3]. We then demonstrate the performance of MILIS for MIL classification on four real-world data sets. To show the generality of the method, we use two binary classification tasks, namely, drug activity detection and infested plant pathogen detection in hyperspectral imagery. We also used two multiclass classification settings, region-based image classification and object class categorization.

For all of our experiments, we have fixed the number of iterations of MILIS to 5. The number of iterations was set empirically as a trade-off between the convergence of optimization and performance improvement. The feature mapping parameter γ in (2) as well as the SVM regularization parameter C was chosen via five-fold cross validation on the training data using grid search. The scale parameter β for KDE in (4) was fixed to be equal to γ for both binary and multiclass MIL problems. For drug activity detection and region-based image retrieval, we compare the training time of MILIS with the alternative MILES algorithm. The code has been implemented in Matlab with the key routines of instance selection/updating and classifier training written in C++. For the KNN search involved in density estimation, we have used ANN, a C++ library for approximate nearest neighbor searching¹ and empirically set the number of neighbors k to 10. In practice, we find that the results of instance selection are not very sensitive to the choice of k provided k is on the order of 10.

The experiments were conducted on a PC with a 3.0 GHz Intel Core 2 Duo CPU and 4 GB of memory. All algorithms (including MILIS, MI-SVM, mi-SVM, and MILES) were implemented in-house, making use of the LIBSVM C++ package for training the two-norm SVMs [24].² LIBSVM solves the standard SVM using sequential minimal optimization [21]. We apply LIBSVM only in the first iteration of SVM training to provide an initial value for SVM weights. Subsequent steps use stochastic gradient descent [31] to update the SVM weights in an incremental fashion. For the MILES and MILIS_{L1} implementations, we have used the MOSEK optimization package³ so as to solve the LP arising from the one-norm SVMs. Note that although the results in [4] were obtained using the CPLEX software for solving the LP, the computation times will ultimately be dependent on the size of the MIL problem at hand. Since complexity grows as a function of the training instance data set, it may not be possible to consistently rely on the power of a fast LP solver to tackle increasingly complex problems arising in the MILES setting [4]. It is worth noting here that we tested other LP packages at our disposal, including the linprog routine in the Matlab optimization toolbox, the GNU Linear Programming Kit (GLPK), and PCx.⁴ We found that none of them could outperform the speed of MOSEK in our experiments.

¹ The package can be downloaded at <http://www.cs.umd.edu/~mount/ANN/>.

² The package can be downloaded at <http://www.csie.ntu.edu.tw/~cjlin/libsvm/>.

³ For more information, visit <http://www.mosek.com/>.

⁴ For more information on PCx, visit <http://pages.cs.wisc.edu/~swright/PCx/>.

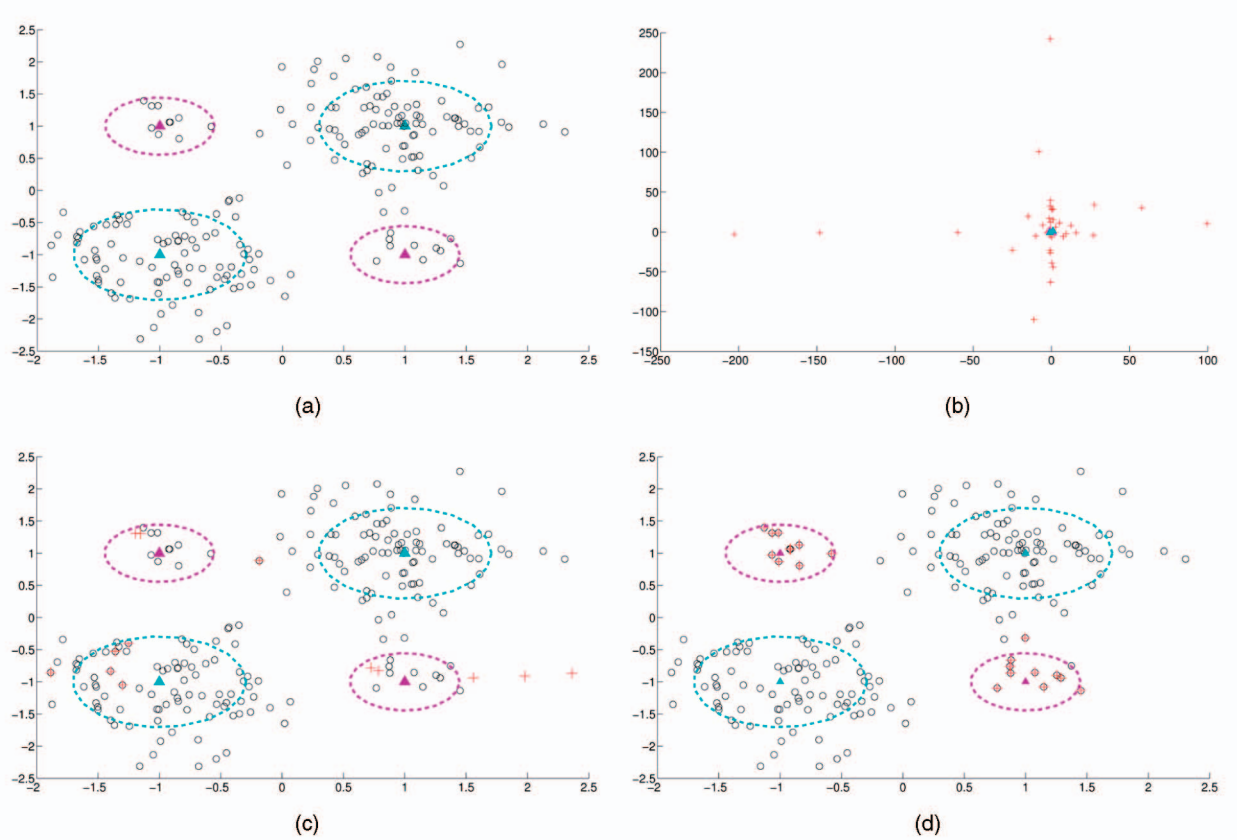


Fig. 4. Example results of instance selection on synthetic data. (a) Raw data. (b) EM-DD. (c) EM-DD close-up view. (d) MILIS.

6.1 Synthetic Data Results

We commence by illustrating the ability of instance selection via MILIS for the synthetic data set shown in Fig. 4. We have generated a data set of 20 positive bags and 20 negative ones, with five instances in each bag. The instances are represented by circles in Fig. 4a. There is only a single positive instance in each positive bag. The positive instances are randomly drawn from a mixture of Gaussians (MoGs) with two components, as shown in broken magenta curves in Fig. 4a. The negative instances are drawn from a different MoG distribution with two Gaussian components shown in broken cyan curves. The solid triangles show the center locations of the respective Gaussian components. Fig. 4b shows the IPs extracted by EM-DD [6] in red plus signs. We can see that a large amount of IPs lie further away from the data distribution. This is due to the nonconvexity of the EM-DD cost function, which is likely to generate outliers with high likelihood value. Fig. 4c provides a close-up view of the IPs yielded by EM-DD. Fig. 4d shows the IPs selected by the nonparametric KDE approach in MILIS. We can see that MILIS has successfully selected the single positive instance from each positive bag as the initial IP. This is in contrast to the fact that the initial IPs selected by EM-DD are not as discriminative as those of MILIS with many miss-hits. Moreover, MILIS takes less than 0.1 second for initial instance selection on this data set and is much more efficient than EM-DD, which takes more than 15 seconds and thus can be impractical for large-scale applications.

We also examined the effect of initialization on MILIS. In fact, we found that it is not overly sensitive to initialization, which is illustrated on the same data set. We deliberately initialize all IPs to the negative instances. After five iterations, the majority of the IPs are updated to the positive instance with classification error dropping to 0. This process is shown in Fig. 5, where the top left panel shows the plots for the initial IPs. Those in the last iteration and the cost function value/error rate as a function of iteration number are shown on the bottom row. Intermediate IPs for iterations 1, 3, and 5 are shown in the remaining panels.

6.2 Drug Activity Detection

In our second experiment, we test MILIS on the two musk data sets, MUSK1 and MUSK2, for drug activity prediction. These are the standard benchmark data sets for testing MIL algorithms. Both data sets are accessible from the UCI Machine Learning Repository.⁵ The data set MUSK1 contains 92 bags, with 47 of them being positive and the remaining 45 being negative. The data set has an average of 5.17 instances in each bag. The data set MUSK2 contains 102 bags, where 39 of them are positive and the remaining ones are negative, with each bag having an average of 64.70 instances. Table 1 reports the classification results measured in terms of the mean prediction accuracy of 10-fold cross validation. Here, we have tested standard MILIS and its variant using one-norm SVM as the classifier, termed MILIS_{L1} in the table. We have also tested MILES,

5. <http://www.ics.uci.edu/~mlearn/MLRepository.html>.

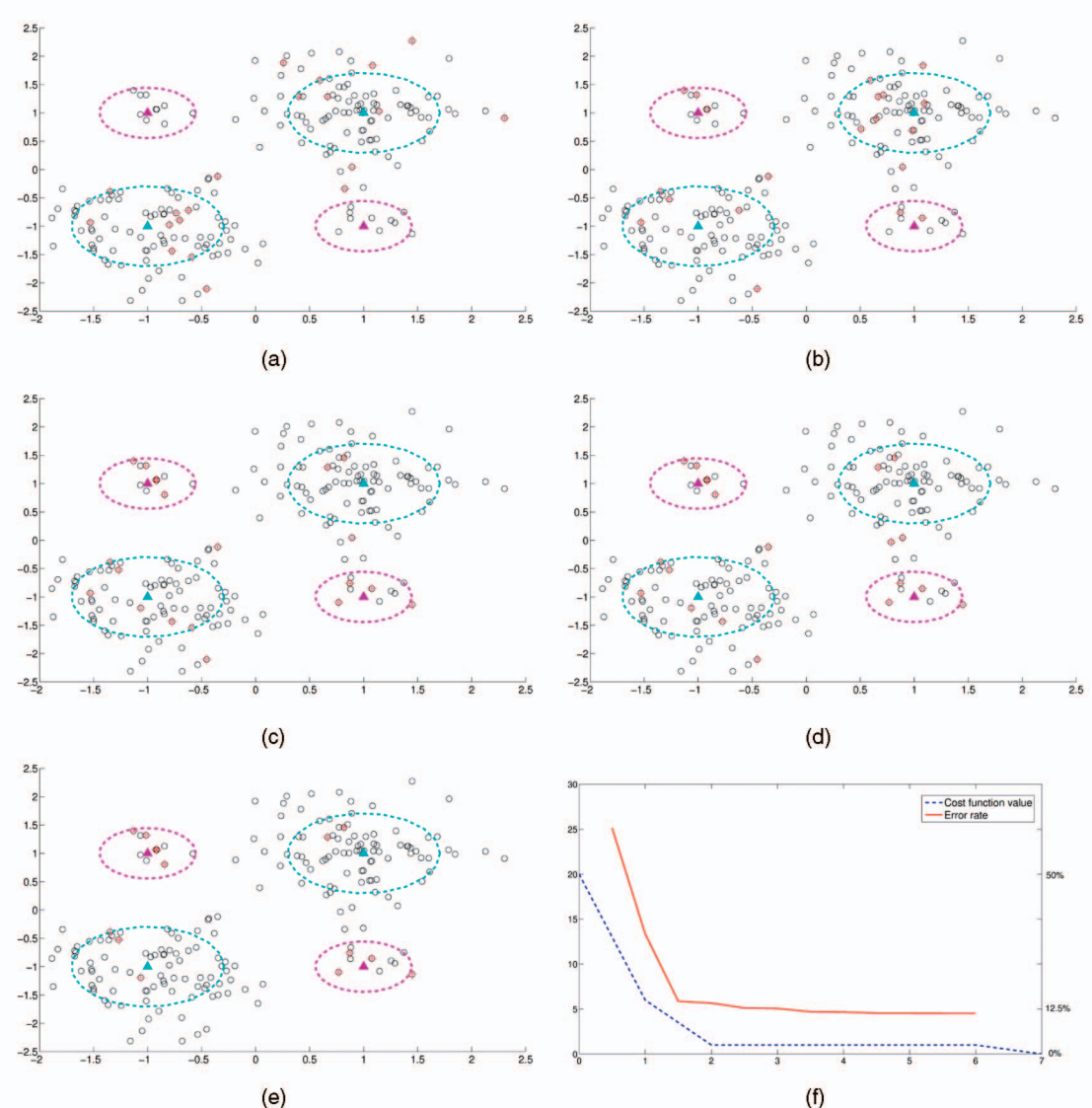


Fig. 5. Behavior of IPs as a function of iteration number for poor algorithm initialization. (a) Initial step. (b) Iteration 1. (c) Iteration 3. (d) Iteration 5. (e) Final result. (f) Cost (y-axis) versus iteration number (x-axis).

TABLE 1
Performance Comparison of the MILIS Algorithm
and the Alternatives on the MUSK Data Sets

Algorithm	MUSK1	MUSK2
MILIS	88.6: [85.8, 91.5]	91.1: [89.4, 92.8]
MILIS _{L1}	85.6: [82.5, 88.7]	88.8: [87.2, 90.4]
MILES [4]	86.3: [84.9, 87.7]	87.6: [86.2, 89.2]
MI-SVM [11]	83.8: [82.6, 84.9]	86.5: [85.0, 88.0]
mi-SVM [11]	88.0: [87.0, 88.0]	88.4: [87.0, 89.8]
DD-SVM [3]	85.8	91.3
APR [1]	92.4	89.2
DD [5]	88.9	82.5
EM-DD [6]	84.8	84.9

MI-SVM, and mi-SVM, and report, in square brackets, the mean cross-validation accuracy averaged over 15 different random runs and the 95 percent confidence interval. For the sake of completeness, we have also included results for other MIL methods in [4]. From Table 1, we can observe that MILIS delivers better performance in terms of higher classification accuracies as compared with those yielded by MILES and other alternatives.

In Table 2, we report the timing results for MILIS and the alternatives. The speedup of MILIS over MILES for the MUSK2 data set is more obvious due to the large number of instances. As mentioned before, the main obstacle to the efficiency of MILES is in the training of the one-norm SVM, which could be very costly for a large number of instances and leads to the big difference in training speed for the two methods under study. This is also corroborated by the training speed of MILIS_{L1}, where the one-norm SVM classifier takes more time in training than that used for the “standard” MILIS. MI-SVM and mi-SVM are faster than MILES but still slower than MILIS when applied to the

TABLE 2
Comparison of Training Speed, in Seconds, for the MUSK Data Sets

Algorithms	MILIS	MILIS _{L1}	MILES	MI-SVM	mi-SVM
MUSK1	0.2 ± 0.1	0.6 ± 0.2	2.6 ± 0.4	0.25 ± 0.05	0.3 ± 0.1
MUSK2	6.8 ± 2.0	12.8 ± 1.0	691.9 ± 292.3	8.3 ± 0.8	13.2 ± 1.8

MUSK2 data set. This is because they treat the SVM classification problem at the instance level. At each iteration, mi-SVM learns an SVM in the instance feature space using all input instances as the training set. MI-SVM trains a similar SVM by using all negative instances and a single positive instance in each positive bag. Thus, their computational cost increases greatly when the data set contains a large number of instances per bag, which is the case for the MUSK2 data set.

Next, we examine the influence of different initialization strategies on the performance of MILIS. Besides the initialization using KDE as discussed in Section 4.2, we can also initialize MILIS in three different ways. In the first of these, the initial IPs are selected randomly from the training bags (RANDOM). The second initialization alternative uses DD values as a guide for the true positivity of the instance (DD). Specifically, let \mathbf{x} be an instance in a bag B from the k th class. We can evaluate its DD value making use of the following equation:

$$\prod_{i,y_i=k} s(B_i, \mathbf{x}) \prod_{i,y_i \neq k} (1 - s(B_i, \mathbf{x})),$$

and select the instance achieving the highest DD value in the bag as the IP. The final strategy for initialization is to simply use all instances in the training bag to form the bag-level feature map (ALL), which is the same as the MILES feature map. The only difference here is that a two-norm SVM classifier is used instead of the one-norm SVM. The SVM can be solved more efficiently in its dual formulation with complexity dependent on the number of bags in the training set. Since all instances are used to form the initial feature mapping, there is no need for instance update and iterative learning though. Table 3 compares the performances achieved by the above-mentioned initialization strategies for MILIS on the MUSK data sets.

From the table, we can see that KDE achieves the highest accuracy, on average, for the MUSK1 data set and is highly competitive with respect to DD initialization for the MUSK2 data set. Moreover, the alternative strategies achieve more or

less comparable classification accuracies for both data sets. However, none of the alternatives produce a consistently better performance on both data sets in comparison with the proposed KDE instance selection method for initialization.

Finally, we examine the sensitivity of the final feature pruning to the cutoff threshold value r with respect to the classification performance as well as the sparsity of the resulting feature map. Fig. 6 shows the classification accuracies in percentage and sparsity values of MILIS against different cutoff values versus those of MILES. Here, the threshold r is a relative cutoff value, which has been set to multiples of the median of the feature weight absolute values. The sparsity values are computed by the average percentage of the final number of IPs corresponding to nonzero weights within the total number of training instances over different training rounds. It can be seen that in contrast to MILES, MILIS not only achieves higher classification accuracies but also generates sparser feature maps for sufficiently, but reasonably, large cutoff values. This leads to higher efficiency in the testing stage. This efficiency of prediction is largely dominated by the time spent on computing the feature map, which is directly relevant to the number of IPs kept after training. We also note that the performance of MILIS is quite insensitive to the choice of cutoff values for a large range of r . Only when $r > 2$ does the performance starts to downgrade noticeably. Hence, in practice, it is quite easy to empirically select a cutoff value that achieves a good trade-off between performance and efficiency. Here, we have set $r = 1$ for all our experiments.

6.3 Plant Pathogen Detection in Hyperspectral Imagery

In this section, we turn our attention to the detection of plant pathogens via hyperspectral imagery. In this application, we are interested in the use of hyperspectral imagery for crop disease detection and mapping. We have taken 120 images of capsicum plants (CAPS), where 60 of them are healthy. The rest of these have been infected with a virus whose visible symptoms are not yet apparent. The left-hand column of Fig. 8 shows sample pseudocolor images for both healthy and infected specimens. From the color alone, there is no noticeable difference between the two. Nevertheless, we can classify them based on their hyperspectral signatures. This is a typical MIL problem where an image is a bag and foreground pixels (i.e., pixels representing plant tissue) are instances in the bag. Healthy plants are referred to as the negative class, whereas infected ones are deemed positive. While healthy plants should have all healthy leaves, not all regions on the infected plant leaves are ill. We use the normalized reflectance at each pixel as the instance-level feature vector. Sample foreground regions for

TABLE 3
Performance Comparison of Different Initialization Methods for MILIS on the MUSK Data Sets

Initialisation method	MUSK1	MUSK2
KDE	88.58 : [85.71, 91.45]	91.09 : [89.42, 92.76]
RANDOM	86.76 : [82.22, 91.30]	90.19 : [89.01, 91.36]
DD	87.03 : [83.76, 90.30]	89.95 : [88.20, 91.70]
ALL	87.07 : [83.37, 90.76]	91.63 : [90.35, 92.92]

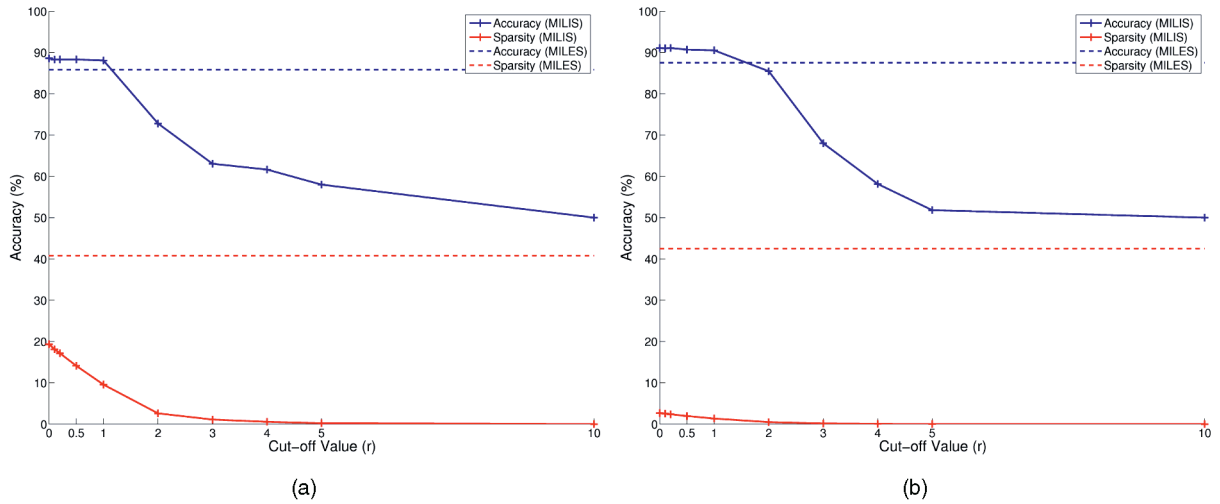


Fig. 6. Influence of final feature pruning on classification performance and sparsity for MILIS on the MUSK data sets. (a) MUSK1. (b) MUSK2.

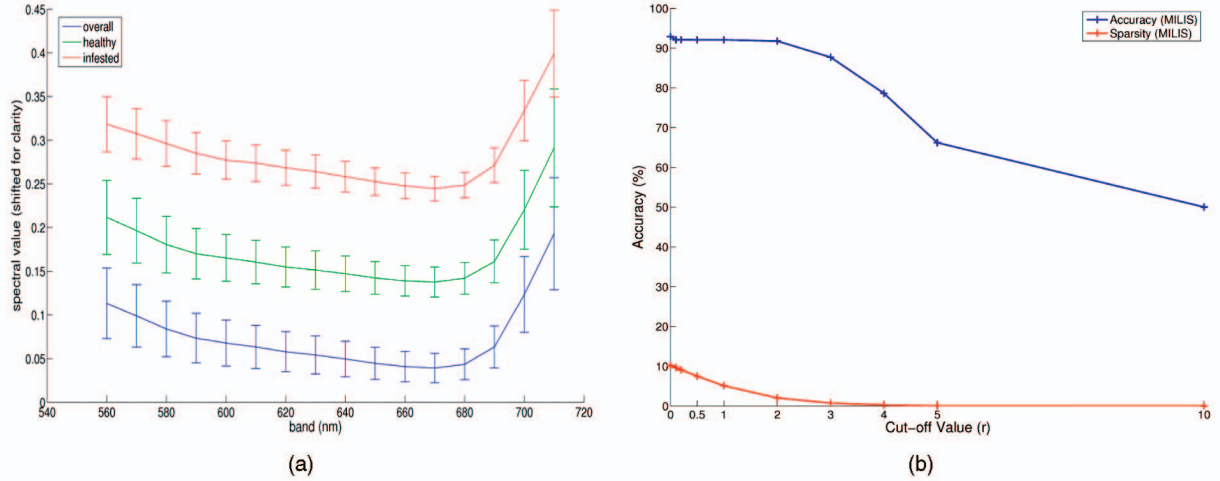


Fig. 7. (a) Mean Spectra for the instance in all bags (blue), positive bags (red), and negative bags (green). (b) Influence of final feature pruning on classification performance and sparsity.

TABLE 4
(a) Classification performance of MILIS on CAPS Data Set
(b) Performance Comparison of Different Initialization Methods for MILIS on the CAPS Data Set

	Accuracy
Infected Class	93.93 : [92.90, 94.96]
Healthy Class	91.24 : [90.09, 92.39]
Overall	92.87 : [92.27, 93.47]

(a)

Initialisation method	Performance
KDE	92.87 : [92.27, 93.47]
Random	92.18 : [91.54, 92.82]
DD	91.59 : [90.69, 92.50]
All	92.67 : [91.82, 93.52]

(b)

the pseudocolor images are shown in the middle column of Fig. 8. In Fig. 7a, we show the mean spectra of all pixels in the ROI for each image, as well as the mean pixel spectra for positive (infected) and negative (healthy) classes. Note that here we have offset the curves for the sake of clarity; otherwise, they would all overlap with each other in the figure. From the average statistics, there is no apparent

existence of patterns that distinguish the positive class from the negative one.

For our experiments, we have randomly divided the image data set into six disjoint subsets with equal number of healthy and infected plants. The ROI of each training image contains an average of 500 pixels, which is equal to the number of instances in each bag. Hence, the dimension of the instance space is over 20,000, making the MILES

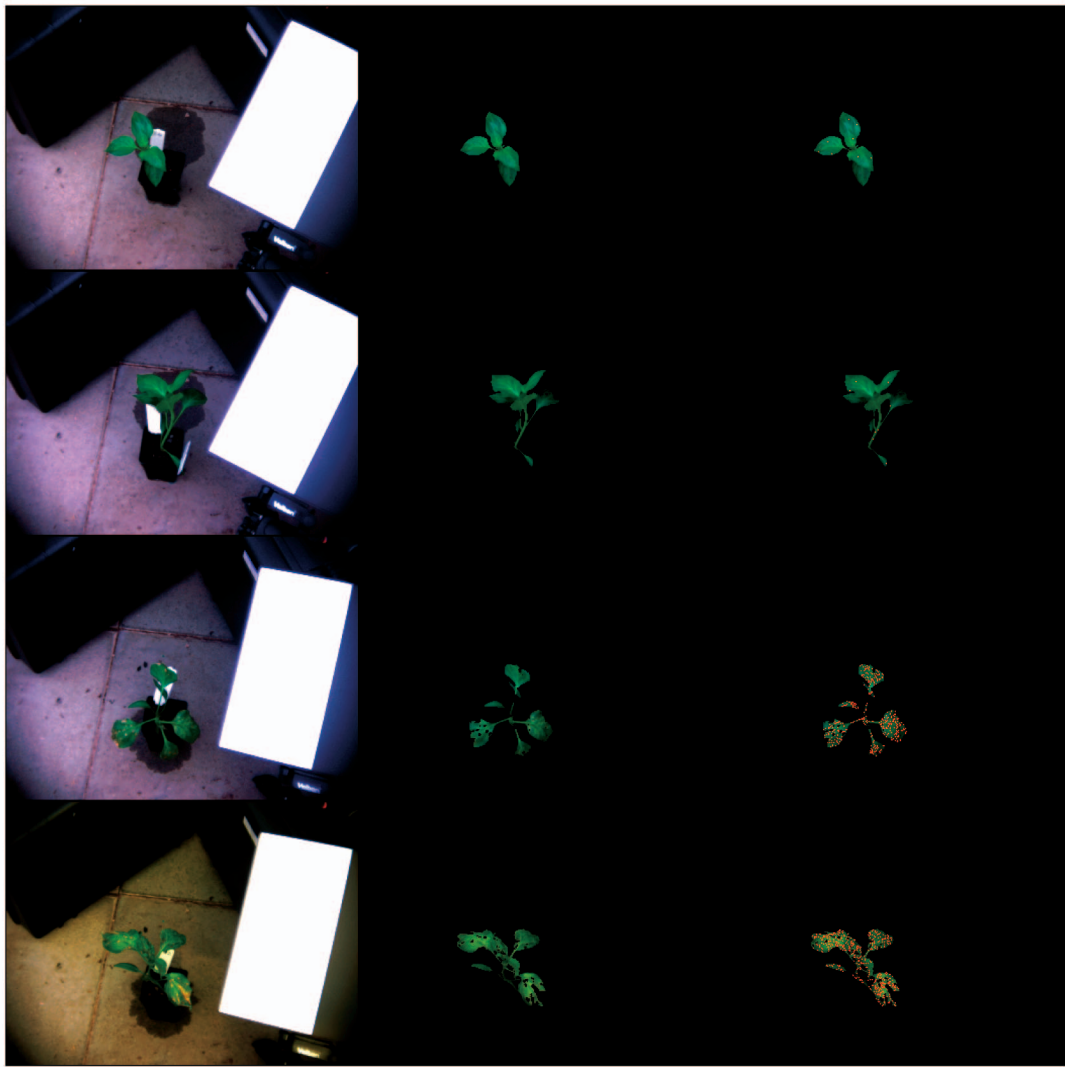


Fig. 8. Example mapping results for the detection of infected regions in hyperspectral imagery from the CAPS data set. Left-hand column: pseudocolor image; middle column: foreground regions; and right-hand column: pathogen mapping results.

embedding overly complex for the problem. Yet, MILIS can still be successfully applied. We applied it to the image data set and measured the average sixfold cross-validation accuracy. The above test is repeated over 10 different random partitions. The mean classification accuracy and the standard deviation are reported in Table 4a. We can see that MILIS is quite effective in detection and achieves an overall accuracy rate of 92.9 percent. It has a low false positive rate and, on average, over 9.1 out of 10 healthy samples are classified correctly. The detection rate for infested plants is higher, with an average about 9.4 out of 10 infested plants will be identified by our approach. Considering the challenging nature of this application, the results are quite encouraging. Note that this trend is consistent with the previous application.

Table 4b reports the performance of different initialization methods, as discussed in the previous section, on the CAPS data set. All four initialization strategies perform quite similarly for this data set, with KDE achieving a margin of improvement on classification accuracy over the alternatives, followed by initialization using all instances and random selection of IPs. Instance selection based on DD values does

not perform as well as expected. Fig. 7b shows the plots for classification accuracy and sparsities versus the cutoff threshold. As before, that classification performance is quite stable for a large range of cutoff values. Within this range, sparsity can be maintained by increasing the cutoff value.

In the rightmost column of Fig. 8, we show the image mapping results rendered by MILIS for both healthy and infested plants. This is achieved by treating each pixel as a bag with singleton instance and applying the learned classifiers at pixel level. The first three rows show the mapping results over the ROIs of healthy plants, whereas the last three rows show the mapping results for infected ones. The red pixels in the ROIs denote those that have been classified as infected. It can be clearly seen that MILIS successfully detects infected plants without generating false alarms on the healthy specimens.

6.4 Region-Based Image Categorization

For the purpose of region-based image categorization, we have tested MILIS on the COREL image data set and compared our results with those yielded by MILES. The data set contains 2,000 images taken from 20 different

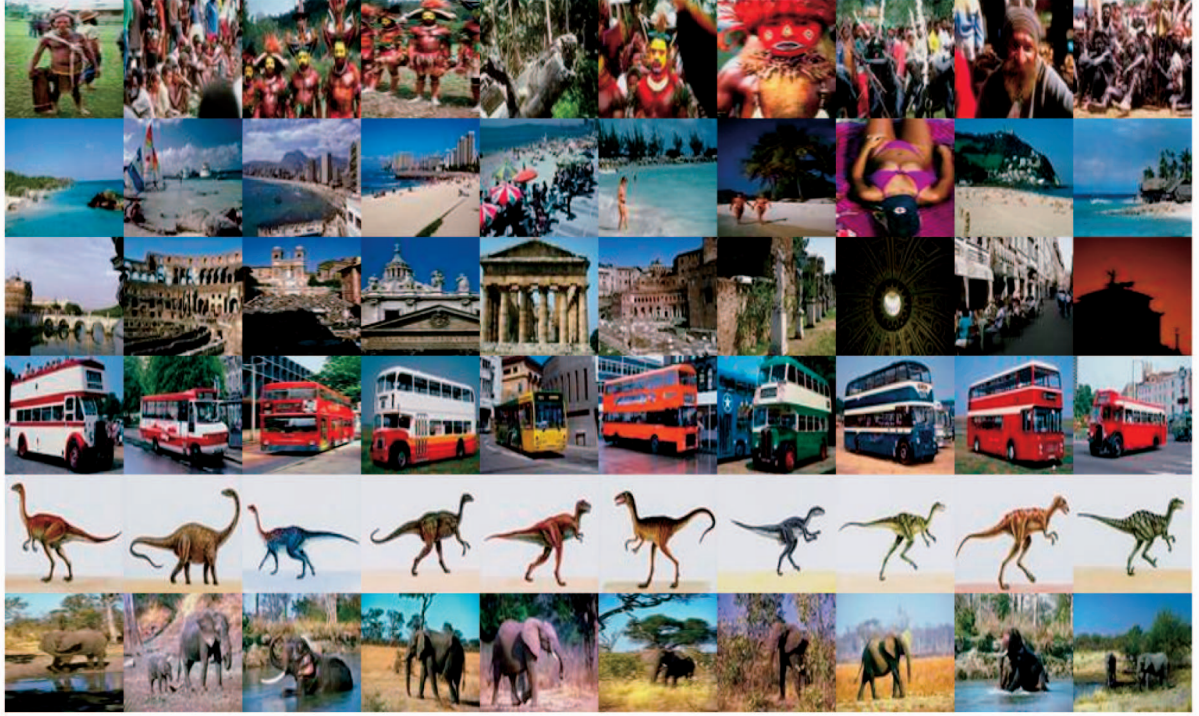


Fig. 9. Example images from the COREL image database used for region-based image categorization.

categories, with 100 images in each class. Some examples of the database images are shown in Fig. 9, where images on the same row are from the same category. This is a multiclass classification problem. Thus, we adopt the one-against-others strategy to train 20 binary SVM classifiers. A test bag is assigned to the category with the largest decision value given by the SVM classifiers. Each image is segmented into several regions and features are extracted from each region. Hence, this is a typical MIL problem with images as bags and region features as instances. Details of segmentation and feature extraction are beyond the scope of this paper and interested readers are referred to [3], [4] for further information of the database.

Two tests have been performed. The first test uses only the first 10 categories in the data set for training and testing, while the second one uses the complete data set with all 20 categories. For both tests, we randomly split all images into 50 percent training and testing data. Training and testing were repeated for five different random partitions. The classification accuracy rates of different algorithms are outlined in Table 5, including the results of DD-SVM as reported in [4].

From the table we can see that the MILIS algorithm is very competitive for image categorization tasks, with a margin of advantage in terms of the accuracy with respect to MILES and MILIS_{L1}, its one-norm SVM variant, followed by MI-SVM and mi-SVM with a large margin of advantage. This is quite encouraging considering the fact that MILES is highly competitive on the COREL image data set [4]. Also, from the results of training speed reported in Table 6, we can see that MILIS is much faster than MILES due to the efficient instance selection and fast classifier learning, and still more efficient than MI-SVM and mi-SVM, which do not

perform very well for classification. From this experiment, we can see that MILIS again outperforms its one-norm SVM variant MILIS_{L1} in both performance and speed. Note that the timing results reported in Table 6 are in seconds spent for the training over all the classes.

We now turn our attention to the influence of initialization and final feature pruning on the performance of MILIS. The results yielded making use of the previously mentioned methods for initialization are shown in Table 7 and Fig. 10. Table 7 shows a slightly different trend as compared to that seen in previous experiments. This time, using all instances to initialize the bag-level feature map does not produce as good classification results as those yielded by the other three methods. Among them, KDE achieves the highest classification accuracy and performs better than other initialization schemes. Moreover, the DD-based selection scheme still

TABLE 5
Image Categorization Accuracy
for the MILIS Algorithm and MILES

Algorithm	1000-Image Data Set	2000-Image Data Set
MILIS	83.8 : [82.5, 85.1]	70.1 : [68.5, 71.8]
MILIS _{L1}	82.5 : [80.8, 84.2]	67.4 : [65.3, 69.4]
MILES [4]	82.3 : [81.4, 83.2]	68.7 : [67.3, 70.1]
DD-SVM [3]	81.5 : [78.5, 84.5]	67.5 : [66.1, 68.9]
MI-SVM [11]	75.1 : [73.2, 77.0]	55.1 : [53.6, 56.5]
mi-SVM [11]	76.4 : [75.3, 77.5]	53.7 : [52.2, 55.2]

TABLE 6
Comparison of Training Speed, in Seconds, for MILIS and the Alternatives Applied to Image Categorization

Algorithms	MILIS	MILIS_{L1}	MILES	MI-SVM	mi-SVM
1000-Image Data Set	7.3 ± 0.5	31.3 ± 0.7	180.3 ± 10.6	9.9 ± 0.8	11.4 ± 0.6
2000-Image Data Set	30.6 ± 3.8	565.0 ± 28.0	960 ± 30.5	55.2 ± 1.4	63.3 ± 2.3

does not show any advantage over random selection. Fig. 10 shows the plots for classification accuracy as well as sparsity as a function of the cutoff threshold. Following the trend in our previous experiments, it can be seen that classification performance is quite stable with a large range of cutoff values. Within this range, more sparse feature maps can be achieved with increasing cutoff values. Here, we can achieve a margin of improvement in classification performance over MILES while maintaining similar level of sparsity with $r = 1$ for both COREL data sets.

Finally, we show some results of the instance selection by MILIS in Fig. 11. For region-based categorization, each IP is a region with discriminant features pertaining its corresponding class. In the figure, we show nine pairs of images on three rows, where each pair consists of the original color image on the left-hand side and the segmentation map on the right-hand panel. Each region in the segmentation map is represented by the same color, whereas the highlighted white-colored regions indicate the regions for which the corresponding instances have been selected as the IPs for classification by the MILIS algorithm. It can be seen that the highlighted regions are indeed in good accordance with the intrinsic features of the class.

6.5 Object Class Categorization

In our last experiment, we have applied MILIS to object class categorization on the Caltech 101 image database [32]. The database contains a total of 8,677 images from 101 classes. Each class contains images from the same objects category. Some example images from the database are shown in Fig. 12. It can be clearly seen that even images for the same object category exhibit large intraclass variance due to shape, pose, and illumination variations. This presents a challenging setting to the recognition task.

Here, we use the discriminative bag-of-words approaches [33], [34], [35] as the baseline. For our experiments, these methods extract and quantize local feature descriptors so as to recover a histogram of codeword occurrences from

the quantized vocabulary as the image level feature. One problem with these approaches is that local features are extracted over the full image and thus inevitably include noisy background features. To tackle this problem, Bosch et al. [36] proposed a method for the automatic extraction of regions of interest (ROI) of the target objects in the images so as to use features within the ROI alone to build frequency histograms. Here, we propose an alternative approach to object categorization based on the MIL technique discussed in this paper. We used multiple histograms of feature descriptors over different local regions of the image to represent the training images. Each local region represented by the histogram is a candidate ROI. If the image contains the target object, then at least one of the candidates should have high likelihood of corresponding to the object under study. Otherwise, all candidate histograms should have low similarity with respect to the specified target. This is a typical multiclass MIL scenario.

For our categorization experiments, we have used a subset of 3,060 images from 102 classes (including a class of background images), with 30 images in each class. The candidate ROI locations are learned from the annotated ROIs for the training images. This is achieved by clustering on the normalized x-y coordinates of the ground truth. A vocabulary of 50 ROI vectors is formed after clustering, each specifying a candidate location of the ROI. For the MILES approach, this leads to over 100,000 instances and a dense feature matrix, which, in memory terms, occupies half a gigabyte of space. On the other hand, MILIS is much more economical memorywise due to its instance selection step.

We use a level-1 spatial histogram representation [34] as the instance level feature vector. For the similarity computation, we used the χ^2 distance, which has been empirically shown to be more appropriate for comparing histograms [34], [35]. We tested our MILIS approach with two alternative single instance learning methods. These are the baseline bag-of-features approach (BOW), where features are taken over the whole image, and bag-of-features with ROI (BOW+ROI), where features are taken over ROIs only. Table 8 lists the classification accuracy for MILIS and the alternatives averaged over 10 trials on different random partitioning of training and testing sets using 15 and 20 training images for each class, respectively.

From the results in Table 8, we can see that MIL outperforms the baseline single instance-based BOW approach and achieves a comparable accuracy rate as BOW+ROI, which is highly competitive for categorization on the 101 image database using single type of features. Nevertheless, note that MILIS does not perform explicit ROI detection for training nor does it use any ROI information in the testing stage. The annotated ground truth is only used at the training stage for learning candidate ROI regions, and does not need ROI information in the testing stage.

TABLE 7
Performance Comparison of Different Initialization Strategies for MILIS on the COREL Data Sets

Strategy	1000-Image Data Set	2000-Image Data Set
KDE	$83.78 : [82.51, 85.05]$	$70.12 : [68.45, 71.79]$
Random	$82.22 : [80.25, 84.19]$	$69.20 : [67.72, 70.67]$
DD	$81.89 : [80.10, 83.68]$	$69.14 : [67.67, 70.61]$
All	$81.51 : [79.68, 83.34]$	$68.57 : [67.04, 70.10]$

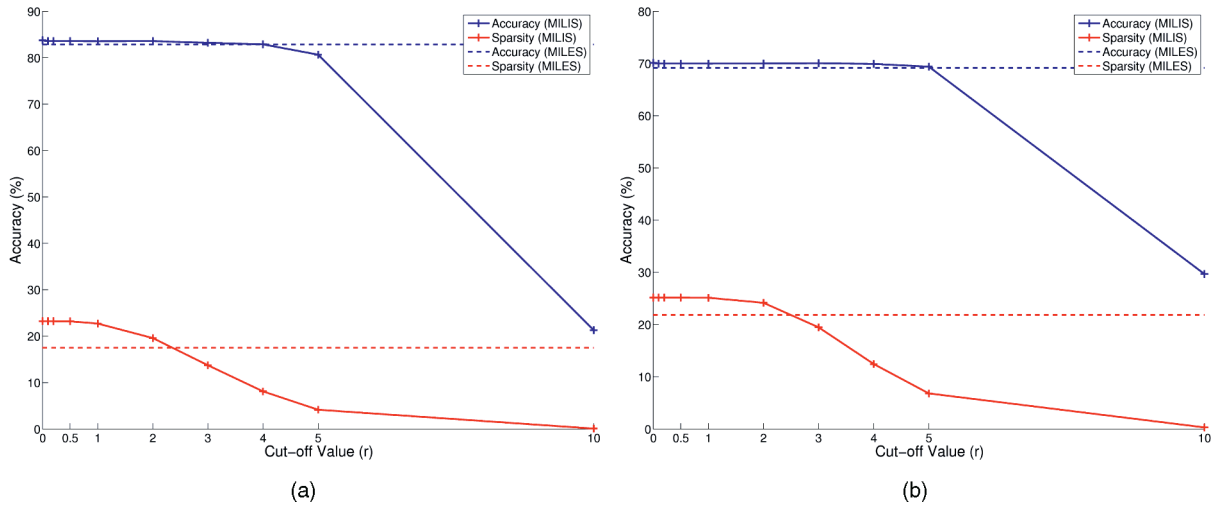


Fig. 10. Influence of final feature pruning on classification performance and sparsity for MILIS on the COREL data sets. (a) 1,000-Image data set. (b) 2,000-Image data set.

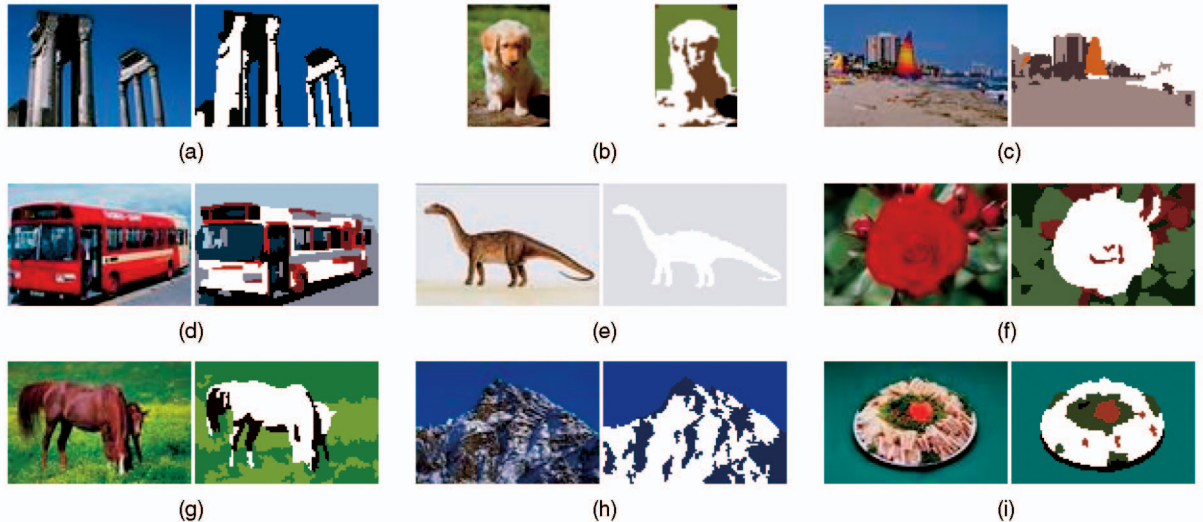


Fig. 11. Sample COREL image data and IPs selected by MILIS: (a) building, (b) dog, (c) beach, (d) bus, (e) dinosaur, (f) flower, (g) horse, (h) mountain, and (i) dish.

However, the IPs selected for the training images do implicitly convey the ROI information. The IPs correspond to instances that carry the discriminant information for the class. Hence, they are likely to be located at the ROIs. Examples of the implicitly selected ROIs corresponding to the IPs are shown in Fig. 13. The ROIs chosen by instance selection are depicted in red rectangles. The ground truth ROIs are enclosed in blue rectangles.

Note that the MIL approach may also be combined with other techniques to further enhance the classification performance. Such methods include, but are not limited to, multiresolution histogram representations, like the pyramid matching kernel [33] and the combination of multiple features for categorization [37].

7 CONCLUSIONS

In this paper, we have presented MILIS, which is an efficient SVM-based multiple instance learning approach to classification. The method is quite general in nature and

hinges on combining instance selection with classifier learning. In this paper, we have also developed an iterative two-step optimization framework to update the classifier. This optimization strategy is guaranteed to convergence. Here, initial instance selection is achieved via kernel density estimation. This is more efficient and effective than the traditional EM-based instance selection strategies. The

TABLE 8
Performance Comparison for the Algorithms under Study

Algorithms	15 images	20 images
MILIS	60.7 : [59.7, 61.7]	63.9 : [63.2, 64.6]
BOW	53.5 : [52.6, 54.4]	56.3 : [55.5, 57.1]
BOW+ROI	60.8 : [59.8, 61.8]	64.2 : [62.7, 65.7]



Fig. 12. Example images from the Caltech 101 image categorization database.

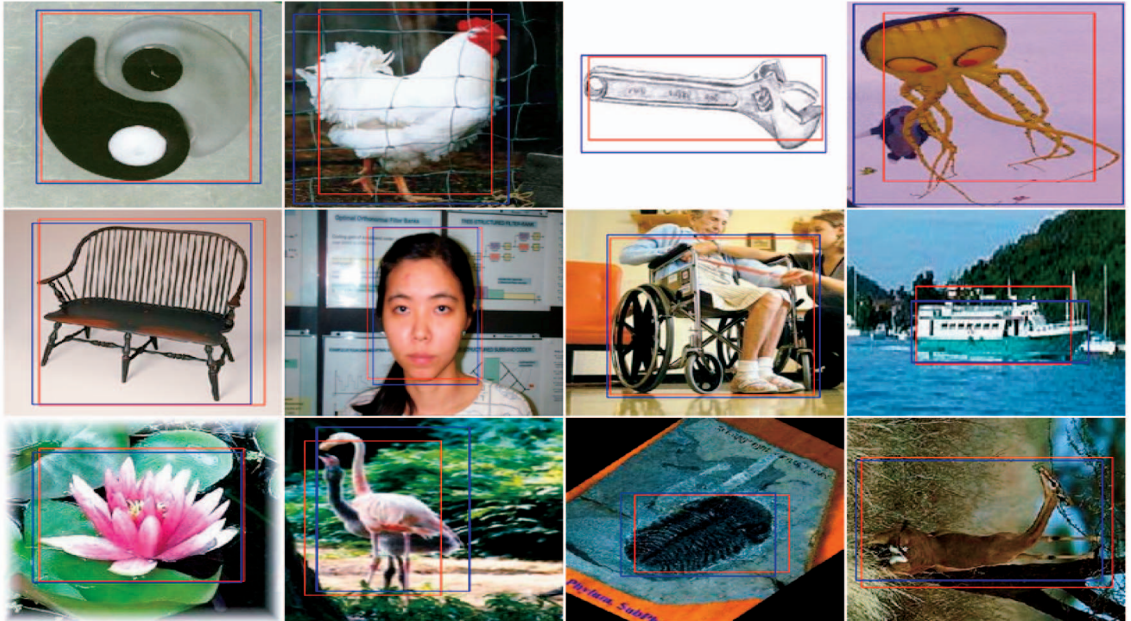


Fig. 13. Examples of implicit ROI selection. Blue rectangles indicate the annotated ground truth, while red rectangles indicate ROIs automatically selected by the MIL algorithm.

proposed approach has demonstrated a margin of improvement over the alternatives. Moreover, as mentioned in the paper, the approach can be applied to a number of classification settings. We have provided results on object recognition and region-based image categorization where MILIS has shown to be more efficient than the competing MIL baseline approach.

There are a number of directions for future research, especially on the topic of initial instance selection. In the

current formulation of MILIS, a single instance is selected from each bag to form the subset of IPs. This is not a condition of the algorithm since any number of IPs can be chosen from each bag for feature mapping. Also note that for negative bags, we have chosen the most negative instance as the initial IP. Since a negative bag only contains negative instances, it would be interesting to explore alternative schemes for IP selection where, for instance, the combination of highly and least likely negatives (near

misses) is used. In addition to IP selection, possible extensions can also be made to classifier learning.

ACKNOWLEDGMENTS

The work presented here was done when Zhouyu Fu was with the National ICT Australia (NICTA). NICTA is funded by the Australian Government as represented by the Department of Broadband, Communications and the Digital Economy, and the Australian Research Council through the ICT Centre of Excellence Program.

REFERENCES

- [1] T.G. Dietterich, R.H. Lathrop, and T. Lozano-Perez, "Solving the Multiple-Instance Problem with Axis-Parallel Rectangles," *Artificial Intelligence*, vol. 89, pp. 31-71, 1997.
- [2] S. Ray and M. Craven, "Supervised versus Multiple Instance Learning: An Empirical Comparison," *Proc. Int'l Conf. Machine Learning*, pp. 697-704, 2005.
- [3] Y. Chen and J.Z. Wang, "Image Categorization by Learning and Reasoning with Regions," *J. Machine Learning Research*, vol. 5, pp. 913-939, 2004.
- [4] Y. Chen, J. Bi, and J. Wang, "MILES: Multiple-Instance Learning via Embedded Instance Selection," *IEEE Trans. Pattern Analysis and Machine Intelligence*, vol. 28, no. 12, pp. 1931-1947, Dec. 2006.
- [5] O. Maron and T. Lozano-Perez, "A Framework for Multiple-Instance Learning," *Proc. Conf. Advances in Neural Information Processing Systems*, pp. 570-576, 1998.
- [6] Q. Zhang and S. Goldman, "Em-DD: An Improved Multiple-Instance Learning Technique," *Proc. Conf. Advances in Neural Information Processing Systems*, pp. 1073-1080, 2002.
- [7] R. Rahmani, S.A. Goldman, H. Zhang, S.R. Cholleti, and J.E. Fritts, "Localized Content Based Image Retrieval," *IEEE Trans. Pattern Analysis and Machine Intelligence*, vol. 30, no. 11, pp. 1902-2002, Nov. 2008.
- [8] J. Wang and J.D. Zucker, "Solving the Multiple-Instance Problem: A Lazy Learning Approach," *Proc. Int'l Conf. Machine Learning*, pp. 1119-1125, 2000.
- [9] B.E. Boser, I. Guyon, and V. Vapnik, "A Training Algorithm for Optimal Margin Classifiers," *Proc. ACM Conf. Computational Learning Theory*, pp. 144-152, 1992.
- [10] T. Gartner, A. Flach, A. Kowalczyk, and A.J. Smola, "Multi-Instance Kernels," *Proc. Int'l Conf. Machine Learning*, pp. 179-186, 2002.
- [11] S. Andrews, I. Tsochantaridis, and T. Hofmann, "Support Vector Machines for Multiple-Instance Learning," *Proc. Conf. Advances in Neural Information Processing Systems*, pp. 561-568, 2003.
- [12] P.-M. Cheung and J.T. Kwok, "A Regularization Framework for Multiple-Instance Learning," *Proc. Int'l Conf. Machine Learning*, pp. 193-200, 2006.
- [13] Z.-H. Zhou and J.-M. Xu, "On the Relation between Multi-Instance Learning and Semi-Supervised Learning," *Proc. Int'l Conf. Machine Learning*, pp. 1167-1174, 2007.
- [14] O.L. Mangasarian and E.W. Wild, "Multiple Instance Classification via Successive Linear Programming," *J. Optimization Theory and Applications*, vol. 137, no. 3, pp. 555-568, 2008.
- [15] P. Viola, J.C. Platt, and C. Zhang, "Multiple Instance Boosting for Object Detection," *Proc. Conf. Neural Information Processing Systems*, 2005.
- [16] S.R. Cholleti, S.A. Goldman, and R. Rahmani, "Mi-Winnow: A New Multiple-Instance Learning Algorithm," *Proc. Int'l Conf. Tools with Artificial Intelligence*, pp. 336-346, 2006.
- [17] Z. Fu and A. Robles-Kelly, "Fast Multiple Instance Learning via $l_{1,2}$ Logistic Regression," *Proc. Int'l Conf. Pattern Recognition*, 2008.
- [18] J. Zhu, S. Rosset, T. Hastie, and R. Tibshirani, "1-Norm Support Vector Machines," *Proc. Conf. Neural Information Processing Systems*, 2003.
- [19] R.O. Duda and P.E. Hart, *Pattern Classification*. Wiley, 2000.
- [20] S. Arya, D.M. Mount, N.S. Netanyahu, R. Silverman, and A.Y. Wu, "An Optimal Algorithm for Approximate Nearest Neighbor Searching Fixed Dimensions," *J. ACM*, vol. 45, no. 6, pp. 891-923, 1998.
- [21] J. Platt, "Probabilistic Outputs for Support Vector Machines and Comparison to Regularized Likelihood Methods," *Advances in Large Margin Classifiers*, pp. 61-74, MIT Press, 2000.
- [22] O. Chapelle, "Training a Support Vector Machine in the Primal," *Neural Computation*, vol. 19, pp. 1155-1178, 2007.
- [23] T. Joachims, "Training Linear SVMs in Linear Time," *Proc. ACM Conf. Knowledge Discovery and Data Mining*, 2006.
- [24] R.E. Fan, K.W. Chang, C.J. Hsieh, X.R. Wang, and C.J. Lin, "LIBLINEAR: A Library for Large Linear Classification," *J. Machine Learning Research*, vol. 9, pp. 1871-1874, 2008.
- [25] A. Dempster, N. Laird, and D. Rubin, "Maximum-Likelihood from Incomplete Data via the EM Algorithm," *J. Royal Statistical Soc. Series B (Methodological)*, vol. 39, pp. 1-38, 1977.
- [26] T. Minka, "Expectation-Maximization as Lower Bound Maximization," 1998.
- [27] I. Guyon, J. Weston, S. Barnhill, and V. Vapnik, "Gene Selection for Cancer Classification Using Support Vector Machines," *Machine Learning*, vol. 46, nos. 1-3, pp. 389-422, 2002.
- [28] T. Hastie and R. Tibshirani, "Classification by Pairwise Coupling," *Proc. Conf. Advances in Neural Information Processing Systems*, vol. 10, 1998.
- [29] R. Rifkin and A. Klautau, "In Defense of One-vs-All Classification," *J. Machine Learning Research*, vol. 5, pp. 101-141, 2004.
- [30] K. Crammer and Y. Singer, "On the Algorithmic Implementation of Multiclass Kernel-Based Vector Machines," *J. Machine Learning Research*, vol. 2, pp. 265-292, 2001.
- [31] L. Bottou and O. Bousquet, "The Tradeoffs of Large Scale Learning," *Proc. Conf. Advances in Neural Information Processing Systems*, vol. 20, pp. 161-168, 2008.
- [32] L. Fei-Fei, R. Fergus, and P. Perona, "Learning Generative Visual Models from Few Training Examples: An Incremental Bayesian Approach Tested on 101 Object Categories," *Proc. IEEE CVPR Workshop Generative-Model Based Vision*, 2004.
- [33] K. Grauman and T. Darrell, "The Pyramid Match Kernel: Efficient Learning with Sets of Features," *J. Machine Learning Research*, vol. 8, pp. 725-760, 2007.
- [34] S. Lazebnik, C. Schmid, and J. Ponce, "Beyond Bags of Features: Spatial Pyramid Matching for Recognizing Natural Scene Categories," *Proc. IEEE Conf. Computer Vision and Pattern Recognition*, 2006.
- [35] J. Zhang, M. Marszałek, S. Lazebnik, and C. Schmid, "Local Features and Kernels for Classification of Texture and Object Categories: A Comprehensive Study," *Int'l J. Computer Vision*, vol. 73, no. 2, pp. 213-238, 2007.
- [36] A. Bosch, A. Zisserman, and X. Munoz, "Image Classification Using ROIs and Multiple Kernel Learning," *Int'l J. Computer Vision*, 2008.
- [37] M. Varma and D. Ray, "Learning the Discriminative Power-Invariance Trade-Off," *Proc. Int'l Conf. Computer Vision*, 2007.



Zhouyu Fu received the BEng degree from Zhejiang University in 2001, the MEng degree from the Institute of Automation, the Chinese Academy of Sciences, in 2004, and the PhD degree from the College of Computer Science and Engineering, the Australian National University, in 2009. He is currently a postdoctoral research fellow in the Gippsland School of Information Technology, Monash University. His research interests include pattern recognition, machine learning, computer vision, and multimedia information retrieval.



Antonio Robles-Kelly received the BEng degree in electronics and telecommunications in 1998 and the PhD degree in computer science from the University of York in 2003. In 2001, as a graduate student at York, he visited the University of South Florida as part of the William Gibbs/Plessey Award to the best research proposal to visit an overseas research lab. After receiving the doctorate degree, he remained in York until December 2004 as a research

associate under the MathFit-EPSRC framework. In 2005, he took a research scientist appointment with National ICT Australia (NICTA) at the Canberra Lab. Together with this appointment, he became an adjunct research fellow at the Australian National University (ANU). After working on surveillance systems with query capabilities, in 2006, he was appointed project leader of the Spectral Imaging and Source Mapping (SISM) Project and promoted to senior researcher. He has also been a postdoctoral research fellow of the Australian Research Council and currently serves as a conjoint senior lecturer at the University of New South Wales at the Australian Defence Force Academy (UNSW@ADFA). He has been a chair, cochair, and technical committee member of mainstream computer vision and pattern recognition conferences such as BMVC, ICCV, CVPR, ECCV, ACCV, and ICPR. He is also an associate editor of *IET Computer Vision* and the *Pattern Recognition*. His research interests include computer vision, statistical pattern recognition, spectral imaging, and computer graphics. He is a senior member of the IEEE.



Jun Zhou received the BS degree in computer science and the BE degree in international business from Nanjing University of Science and Technology, China, in 1996 and 1998, respectively, the MS degree in computer science from Concordia University, Montreal, Canada, in 2002, and the PhD degree from the University of Alberta, Edmonton, Canada, in 2006. Since 2007, he has been a researcher in the Canberra Research Laboratory, National ICT Australia

(NICTA). At the same time, he is an adjunct lecturer in the College of Engineering and Computer Science, the Australian National University, Canberra, and a conjoint lecturer in the School of Engineering and Information Technology, the University of New South Wales at the Australian Defence Force Academy, Canberra. His research interests include pattern recognition, computer vision, spectral imaging, and machine learning with human-in-the-loop. He is a member of the IEEE.

▷ For more information on this or any other computing topic, please visit our Digital Library at www.computer.org/publications/dlib.